

Frequency Compound Imaging of Defects in Metal Plate Using Airborne Ultrasound with Nonlinear Effect

Ayumu Osumi^{1*}, Fumiya Hamada², Kyosuke Shimizu², and Youichi Ito¹ (¹Coll. of Sci. & Tech., Nihon Univ.; ²Grad. of Sci. & Tech., Nihon Univ.)

1. Introduction

We have studied the non-contact and non-destructive testing method using a scanning airborne ultrasound source technique (SAS) and a harmonic imaging (HI)¹⁻³. One of the improving method of the defect visualization in a non-destructive testing is a frequency compound method^{4,5}. In this report, we investigated to image the defect of the metal plate using the frequency compound method and the HI.

2. Measurement principle

We have proposed to apply the airborne ultrasounds with the nonlinear effects to the non-destructive testing. The Lamb waves with harmonic components are propagated in the metal plate generated by airborne ultrasounds with the nonlinear effects. Note that the nonlinear effects of high-intensity airborne ultrasounds are used to generate the Lamb waves with the harmonic components in the metal plate.

We performed the HI in the metal plate by the Lamb waves with harmonic components. The frequency compound method is the image processing technology to synthesize the image of the various frequencies. This technology realizes improving a lateral resolution and an image uniformity.

In this report, we performed the frequency compound using the Lamb waves with the harmonic components in the metal plate.

3. Experimental equipment and method

Figure 1 shows the schematic of the experimental equipment. The equipment was composed of a high-intensity focused airborne ultrasound source, an acoustic guide, an amplifier (HAS 4051: NF), a synthesizer (WF1974: NF), an acoustic emission (AE) sensor (PICO: Physical Acoustics), a signal amplifier (2/4/6C: MISTRAS), a data logger (USB-6363: NI) and the PC that controls the peripheral equipment.

The sound source was composed of 335 ultrasound emitters arranged on part of the spherical surface with the diameter of 150 mm.

In addition, the sound waves were irradiated through the acoustic guide consisting of the acoustic

window (acrylic; thickness: 2 mm) and the pipe (acrylic; length: 50 mm; inner diameter: 6 mm) to prevent the effects of side lobes. The sound source was driven with the applied voltage of 45 V_{pp}, the frequency of 40.8 kHz, and the sinusoidal wave of 10 cycles. The sound waves irradiated under the above conditions contained integer-order harmonics in addition to the driving frequency because of the nonlinear effects. Using this sound waves, the HI can be performed.

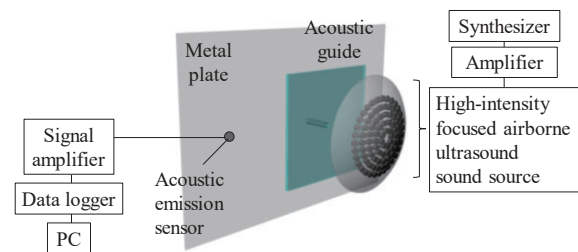


Fig. 1 Schematic of experimental equipment.

Figure 2 shows the schematic of the sample used in this experiment. A duralumin sample was the dimensions of 500 × 340 × 3 mm. The defect area of the depth of 0.5 mm from the surface was the dimensions of 20 × 20 mm. Measurements were performed as follows. High-intensity focused sound waves from the sound source were irradiated to each position of the scanning area shown in Fig. 2 at intervals of 2 mm to generate the Lamb waves in the sample.

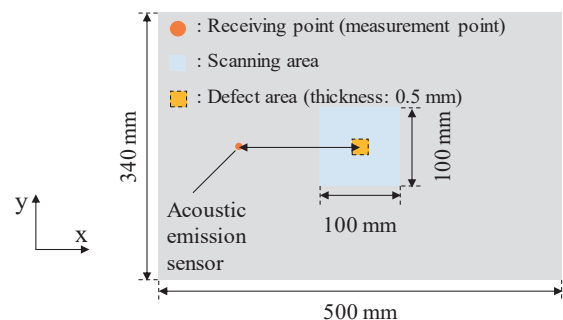


Fig. 2 Schematic of sample.

The vibration waveforms of the Lamb waves were acquired by the AE sensor placed at the measurement point shown in Fig. 2. The driving frequency (40.8 kHz), and integer-order harmonics of the driving frequency were extracted from the

E-mail: *osumi.ayumu@nihon-u.ac.jp

vibration waveforms of the Lamb waves using a bandpass filter. The measurement conditions were the sampling frequency of 2 MHz, the sampling time of 5 ms, and the averaging process of 8 times.

Finally, the frequency compound was performed as follows. Each vibration amplitude distribution was constructed by the peak of the vibration amplitude at each harmonic component. Next, we performed the addition on the vibration amplitude distributions at each harmonic component. In addition, each result was normalized and then added.

4. Results

Figure 3 shows the vibration amplitude distributions at each harmonic component.

As the results, the defect area is visualized by the vibration mode generated in the defect area. In addition, the vibration mode in the defect area is the complex vibration mode as a frequency is higher. However, the vibration mode is also generated in the white frame area in these results. These vibration modes are caused by the interference of the transmitted wave from a vibration point (a measurement point in Fig. 2) and the refracted wave at the boundary between a health area and the defect area.

Figure 4 shows the result of applying the frequency compound. This result is summed the results from the second harmonic to the seventh harmonic.

As the result, similar to the results shown in Fig. 3, the vibration mode is generated in the defect area. However, the vibration amplitude of the interference area in Fig. 4 is smaller than that of the interference area in Fig. 3. Therefore, as shown in Fig. 4, the vibration amplitude in the defect area increases relatively.

5. Conclusion

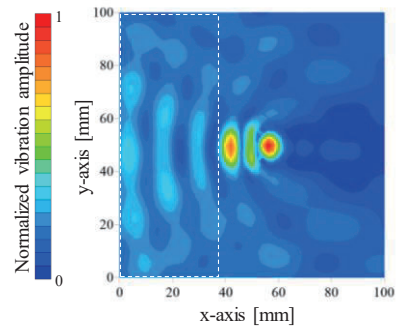
In this report, we investigated to image the defect in the metal plate using the frequency compound method and the HI. As the results, we demonstrated the effectiveness of the frequency compound method and the HI.

Acknowledgment

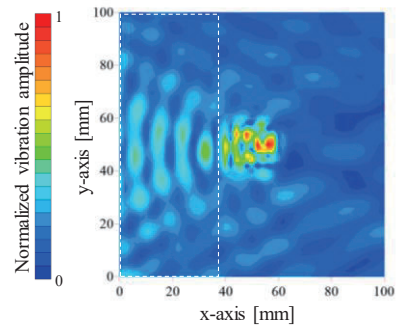
This work was partly supported by JSPS KAKENHI Grant number 22K04624.

References

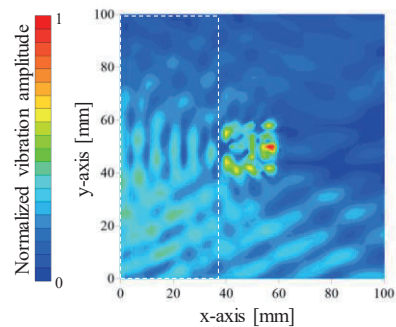
- 1) A. Osumi et al, Jpn. J. Appl. Phys., 58, SGGB14, 2019.
- 2) A. Osumi et al, Acoust. Sci. Technol. 41, pp.885-890, 2020.



(a) 1st.



(b) 2nd.



(c) 3rd.

Fig. 3 Vibration amplitude distributions at each harmonic component.

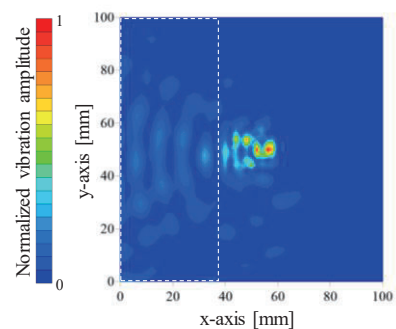


Fig. 4 Vibration amplitude distribution by applying frequency compound.

- 3) K. Shimizu et al, Jpn. J. Appl. Phys., 59, SKKD15, 2020.
- 4) P.A. Magnin et al, Ultrason. Imaging, 4, pp.267-281, 1982.
- 5) I. Akiyama et al, Jpn. J. Appl. Phys., 44, pp.4631-4636, 2005.